

1 Distributed representations of protein domains and genomes 2 and their compositionality

3 A. Viehweger ¹⁻³, S. Krautwurst ¹, B. König ², M. Marz ¹

4 (1) Bioinformatics

5 Faculty of Mathematics and Computer Science

6 Friedrich Schiller University Jena

7 Leutragraben 1

8 07743 Jena

9 (2) Institute of Medical Microbiology

10 University Hospital Leipzig

11 Liebigstraße 21

12 04103 Leipzig

13 (3) Corresponding author: `adrian.viehweger@uni-jena.de`

14 Abstract

15 Learning algorithms have at their disposal an ever-growing number of metagenomes for biomining and
16 the study of microbial functions. We propose a novel representation of *function* called **nanotext** that
17 scales to very large data sets while capturing precise functional relationships.

18 These relationships are learned from a corpus of 32 thousand genome assemblies with 145 million
19 protein domains. We treat the protein domains in a genome like words in a document, assuming that
20 protein domains in a similar context have similar “meaning”. This meaning can be distributed by the
21 **Word2Vec** embedding algorithm over a vector of numbers. These vectors not only encode function but
22 can be used to predict even complex genomic features and phenotypes.

23 We apply **nanotext** to data from the Tara ocean expedition to predict plausible culture media and
24 growth temperatures for microorganisms from their metagenome assembled genomes (MAGs) alone.
25 **nanotext** is freely released under a BSD licence (<https://github.com/phiweger/nanotext>).

26 Introduction

27 An organism can be reduced to the functions its genome encodes. However, the definition of function
28 and its representation remain elusive^{1,2}. Protein domains in a genome are basic units of function, like
29 words are basic units of “meaning” in a document. Embeddings of protein domains in a vector space are
30 a novel representation that captures even subtle aspects of function. When extended to entire genomes,
31 functional “topics” of these genomes can be inferred, which reflect their current taxonomy. Domain and
32 genome embeddings have many useful properties especially as input to learning algorithms and offer the
33 possibility for use in large scale metagenomic applications such as biomining and genotype-phenotype
34 mapping.

35 In metagenomics, the bottleneck of discovery has shifted from data generation to analysis. Many
36 current sequencing efforts are extremely data-intensive, regularly reconstructing thousands of unknown
37 genomes in a single study³⁻⁸. Gene catalogs compiled from metagenomes have millions to billions
38 of records^{9,10}, many without a documented functional role¹¹. This wealth of data holds tremendous
39 potential, from substantially revising the tree of life¹², the discovery of new enzymes and metabolites for
40 biotechnological use¹³ to predictive models that distinguish diseases based on microbial composition¹⁴.
41 To address these questions, learning algorithms such as *neural nets* are powerful pattern detection
42 tools¹⁵. Learning is most effective when the signal in the data is “stable”, i.e. if given a similar input,
43 the target variable is similar too. Such a stable signal has been found in the functions performed by a
44 microbial community, rather than in its taxonomic makeup^{16,17}, although this view is debated¹⁸. To
45 “fit” metagenome-derived functions into learning algorithms, two questions need to be answered: (1)
46 How is “function” defined? (2) How is it represented?

47 (1) Protein-mediated function can be defined as a sequence of protein domains. Domains are typically
48 identified as highly conserved regions in a multiple alignment of similar protein sequences^{19,20}.
49 Most proteins have two or more domains and the nature of their interactions determines the
50 protein’s function(s)²¹. Although chemically, the basic building blocks of proteins are amino
51 acids, protein domains are arguably the basic units of “meaning”. This is supported by their
52 independent evolution²¹⁻²³ and by the fact that the structure of domains is often more conserved
53 than their amino acid sequence^{20,24}, especially in viruses²⁵.

54 (2) Many representations of function exist. *Zhu et al.* used a network-based approach to assign
55 functional similarity to pairs of genomes on the basis of encoded proteins^{26,27}. Other approaches
56 use direct counts of protein domains to distinguish organisms^{28,29}. Both approaches discard
57 context information, which is very important in bacterial and fungal genomes: Not only are genes

58 frequently co-located in e.g. biosynthetic gene clusters (BGCs)³⁰ or polysaccharide utilisation loci
59 (PULs)³¹, but often they are situated in *polycistronic* open reading frames (ORFs)³². Multiple
60 adjacent ORFs are frequently regulated in concert by expression as a single mRNA³³, adding
61 further context dependence. Count-based representations have another disadvantage; they are
62 high-dimensional and sparse. To encode the count of a protein domain out of the 17 thousand
63 domains in the Pfam database¹⁹, the resulting *one-hot-encoded* vector would have an equal number
64 of dimensions with all elements zero except one. Such sparse vectors can make learning very
65 inefficient.

66 A representation that both preserves the context information and results in dense vectors are *word*
67 *embeddings*^{34,35}. They assign words that occur in similar contexts to similar vectors in vector space.
68 The assumption then is that words with similar vectors have similar “meaning”. Indeed, word embed-
69 dings have been shown to capture precise syntactic and semantic relationships in text such as synonyms.
70 Word embeddings are trained on a large collection of unlabeled texts (*corpus*). Training an embedding
71 results in a vector of numbers for each distinct word in the corpus (*vocabulary*). Different training
72 algorithms exist, the most popular of which is Word2Vec^{36,37}. Several extensions have been developed:
73 For example, character information can be included in the embedding model³⁸ or it can be extended
74 to entire documents to create “topic” vectors^{39,40}. Similar words or topics can be identified using the
75 *cosine similarity* of the associated vectors. Because word and document vectors capture similarity,
76 they are effective as input for learning algorithms and facilitate training. Without such a “language
77 model”, a learning algorithm would have to learn about syntax and semantics in parallel to the actual
78 learning task. However, pretrained embeddings already hold this information.

79 Embeddings have been trained on biological objects such as genes^{41,42}, proteins^{43,44}, chemical
80 structures⁴⁵ and nucleotide sequences^{46–48}. Most of these approaches focus on the primary sequence.
81 However, as discussed above, structure is oftentimes conserved although the underlying sequence is
82 not. Furthermore, many sequence variations do not affect function, but act as noise during training,
83 for example in the case of synonymous single nucleotide polymorphisms (SNPs). In this article,
84 we asked how an organism’s functions might be representable in vector space in such a way as to
85 facilitate downstream learning tasks. To approach this question, we trained a vector representation of
86 protein-mediated function on a large, diverse collection of bacterial genomes and their protein domain
87 annotations. The result is a pre-trained embedding model called **nanotext**. We then investigated
88 which functional aspects are captured by the embedding vectors and finally applied the embedding to
89 several unsolved learning tasks.

90 Results

91 Embeddings of protein domains capture functional relationships

92 To train a protein domain embedding, we aggregated sequences of PFAM domains¹⁹ into a *corpus* of 32
93 thousand bacterial genomes with 145 million annotated domains. The set of domains in the corpus
94 forms the *vocabulary* and is comprised of about 10 thousand domains. Training resulted in a vector
95 *representation* of size 100 for each unique protein domain and genome in the corpus. We make the
96 resulting pre-trained model available as **nanotext**. Each domain vector is comprised of latent features,
97 which describe the associated domain’s functional meaning along multiple dimensions.

98 Protein domain embeddings can distinguish functional context with near-perfect accuracy. Generally,
99 embedding accuracy can be tested using a variety of tasks⁵⁰. However, no single task captures all
100 aspects of the representation, because embeddings capture meaning, and meaning is multifaceted.
101 Specific assessment tasks usually rely on labelled datasets e.g. of synonyms. No such dataset exists for
102 protein domains. We therefore estimate embedding accuracy using the *semantic odd man out* (SOMO)
103 task⁵¹: For a set of words, we try to identify the one that does not “fit” into the context. For example,
104 “Cereal” would be *odd* in a set comprising “Zebra”, “Lion” and “Flamingo”. For each ORF in our
105 corpus with more than one domain, we select a random domain from the vocabulary. The mean of the
106 embedding vectors of this set is then calculated. The “odd” domain is the one with the largest cosine
107 distance to this mean, and in the correct case corresponds to the randomly chosen domain. We achieve
108 a 99.27% accuracy on the SOMO task, which is much higher compared to embeddings generated from
109 natural language texts⁵¹.

110 Many domain vectors cluster according to known functional classes, which we derived from an existing
111 mapping of protein domains to putative enzyme functions²⁰. To visualize clusters, we projected all
112 associated domain vectors into two dimensions using the t-SNE visualization algorithm⁵². We found
113 that many domains cluster according to their enzyme function label (Figure 1), while others do not.
114 This might reflect that many domains have several functions and that those functions can overlap.
115 However, the observed clustering is indicative that the domain embeddings are plausible.

116 Domain vectors can be used to explore *domains of unknown function* (DUF). We illustrate this with
117 a case study of DUF1537: Since its introduction to Pfam as a protein family of unknown function, ex-
118 periments have identified it as ATP-dependent four-carbon acid sugar kinase with now two associated
119 domains – PF07005 and PF17042⁵³. Zhang *et al.* used a gene cooccurrence network to identify “con-
120 served genome neighborhoods”. Querying our embedding model for functionally similar domains to

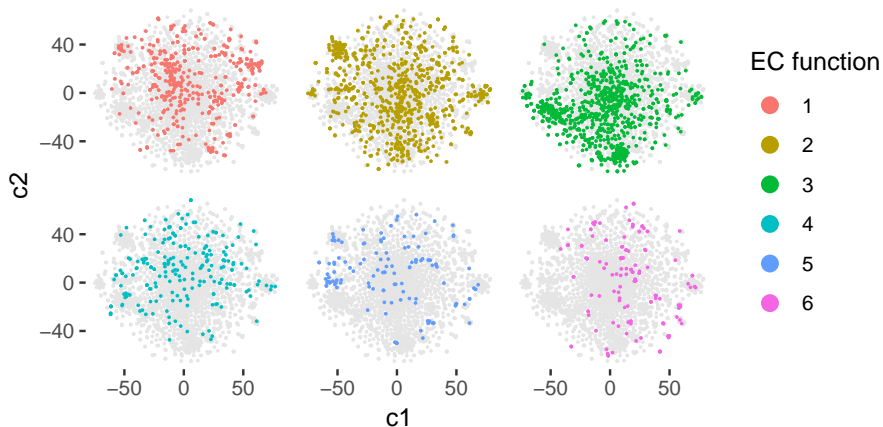


Figure 1: Supplement. Domain vectors cluster according to known functional classes. Projection of the domain vectors from 100 dimensions into two using t-SNE. Some clusters correspond to a single functional class (*enzyme commission* (EC) numbering scheme), which suggests that the learned domain embeddings capture functional relations.

121 PF07005 and PF17042 (because DUF1537 has since been removed), we find exactly the same “conserved”
122 domains as *Zhang et al.* (Table 1). When we query the embedding model with PF07005 (SBD_N) for
123 its closest vector, we find PF17042 (NBD_C) and vice versa, with a cosine similarity of the associated
124 word vectors of 0.93, respectively.

125 Composing domain vectors creates new meaning. A surprising result of the original work on word vec-
126 tors was that they capture linguistic regularities, which can be composed using vector algebra³⁶. For
127 example, vector(“king”) - vector(“man”) + vector(“woman”) is close to vector(“queen”)³⁶. These se-
128 mantic regularities are captured by protein domain embeddings, too. For example, the vector for the en-
129 zyme urease (Urease_beta, PF00699) minus its N-terminal domain (Urease_alpha, PF00449) plus the
130 catalytic domain of ribulose biphosphate carboxylase (large chain, RuBisCO_large, PF00016) results
131 in a vector whose nearest neighbor is the N-terminal domain of the carboxylase (RuBisCO_large_N,
132 PF02788, cosine similarity 0.93).

133 **Functional similarity captures taxonomic properties**

134 A genome can be abstracted as a sequence of protein domains, or by analogy as a document containing
135 words. Embeddings of genomes result in a type of *topic model*⁴⁰ with an associated *topic vector*
136 composed of latent features. The topic of a document might be how much “sports” or “politics” it
137 contains, while the topic of a genome might reflect how anaerobic an organism is or which metabolic
138 constraints it operates under. Note that a topic is merely a cluster of document vectors in embedding

139 space. It is not assigned a label, because it is learned from unlabelled data. We furthermore introduce
140 the term *functional similarity* analogous to nucleotide similarity, to describe the distance between any
141 two genome vectors as measured by their cosine similarity.

142 Genome embeddings can be used to assign genomes to taxa. Unlike protein domain vectors, genome
143 vectors can be inferred for previously unseen, *out of vocabulary* (OOV) genomes. To illustrate this, we
144 used a collection of 957 metagenome assembled genomes (MAGs) based on data from the *Tara Ocean*
145 *Expedition*^{3,7}. These MAGs did not feature in our embedding training set or in reference databases such
146 as RefSeq⁵⁴. Using unknown MAGs imitates the use case of biomining newly sequenced metagenomes.
147 We would expect genome vectors to cluster according to their taxonomy, because organisms with the
148 same taxonomic label frequently share many functions. To visualize this, we projected the genome
149 vectors into two dimensions using t-SNE⁵². We identify clearly delineated clusters that can be assigned
150 to distinct phyla (Figure 2, A). The clustering is hierarchical as to taxonomic rank, in the sense that
151 clusters of e.g. *phyla* are themselves composed of clusters of distinct *classes* (Figure 3, A). Interestingly,
152 many MAGs could not be assigned a taxonomic rank by *Delmont et al.* using marker genes⁷, but have
153 their genome vector cluster clearly with known organisms (Figure 3, B). Genome vectors could be a
154 complement if not replacement for marker gene-based approaches, without the need to select these
155 genes based on prior knowledge⁵⁵.

156 Unlike marker-gene based approaches, genome vectors are remarkably stable when MAGs are incom-
157 plete. From the *Delmont et al.* high-quality, near-complete MAGs, we successively removed an in-
158 creasing percentage of contigs *in silico*, inferred genome vectors, and then identified their nearest
159 neighbors in vector space. We found that the functional similarity of “truncated” genome vectors to
160 their “complete” self decreases only slowly with increasing degrees of incompleteness (Figure 2, B). For
161 an illustrative MAG (TARA_RED_MAG_00040), we find that up to 90% of contigs can be removed until
162 the corresponding genome vector moves notably in embedding space (Figure 2, C). Thus **nanotext**
163 can assign taxonomy to even highly incomplete genomes.

164 Functional and nucleotide similarity are complementary measures of how different two genomes are.
165 For some genomes, both measures correlate (Figure 2, D). However, there are pairs of genomes with
166 low nucleotide similarity but high functional similarity (Figure 2, D). In these cases, both measures
167 offer complementary information. Investigating such a cluster, we found three genomes which in the
168 original study could not be assigned to a taxon below the rank of *domain Bacteria*. Based on functional
169 similarity however, these genomes were clearly related, while they would not have been grouped by
170 their nucleotide similarity alone (Table 2). We could confirm that the three genomes were of the
171 same order *Gemmatimonadales* by searching against a large reference collection of MinHash signatures

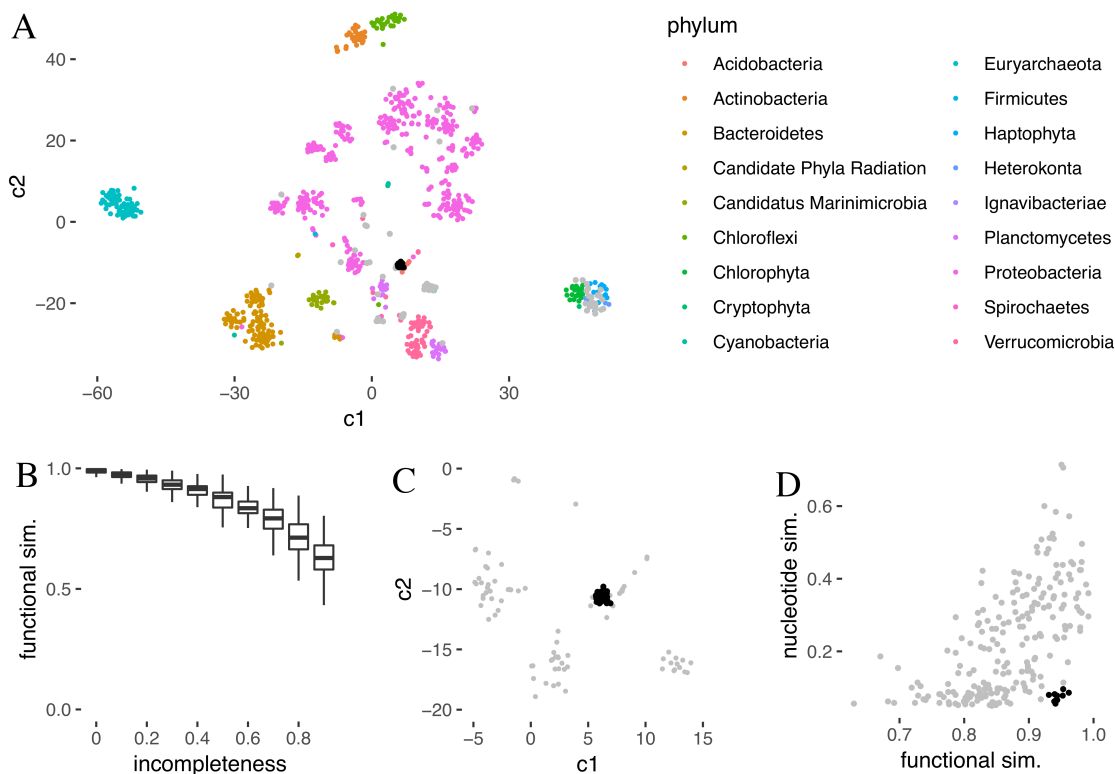


Figure 2: Functional similarity captures taxonomic properties. **(A)** Visualisation of genome vectors using t-SNE projection into two dimensions (components). Clear clusters can be observed which correspond largely to the phylum assigned to the MAGs from which the genome vectors were derived by *Delmont et al.*⁷. Note how archaeal genomes and algae form separate clusters (left turquoise and bottom right, respectively) although the embeddings were only trained on bacterial genomes. **(B)** Detail from (A): The MAG TARA_RED_MAG_00040 was truncated by removing an increasingly large, random subset of its contigs. Then, for each truncated genome, the genome vector was inferred and the closest MAG from *Delmont et al.* marked (black points in (A) and (B)). Remarkably, the truncation has little effect on the placement of the genome vector. Up to 90% of contigs can be removed while the associated genome vector remains in the same region in vector space. **(C)** Effect of MAG truncation on functional similarity: For a random subset of 100 MAGs from *Delmont et al.* we removed an increasing percentage of contigs, calculating the cosine similarity between the truncated genome and the original one. It decreases very slowly as genomes are increasingly truncated. This makes cosine similarity an attractive measure of genome similarity in metagenomic contexts where assembled genomes are more often incomplete than not. **(D)** Pairwise comparison of MAGs from *Delmont et al.* between nucleotide (Jaccard) similarity and functional (cosine) similarity. There are several genomes which are very different in terms of average nucleotide identity as approximated from their k-mer composition using *MinHash*⁵⁶. However, some pairs nevertheless exhibit high functional similarity (black) which suggests similar taxa. Notably, there are no genomes of high nucleotide but low cosine similarity (upper left triangle), which would be implausible.

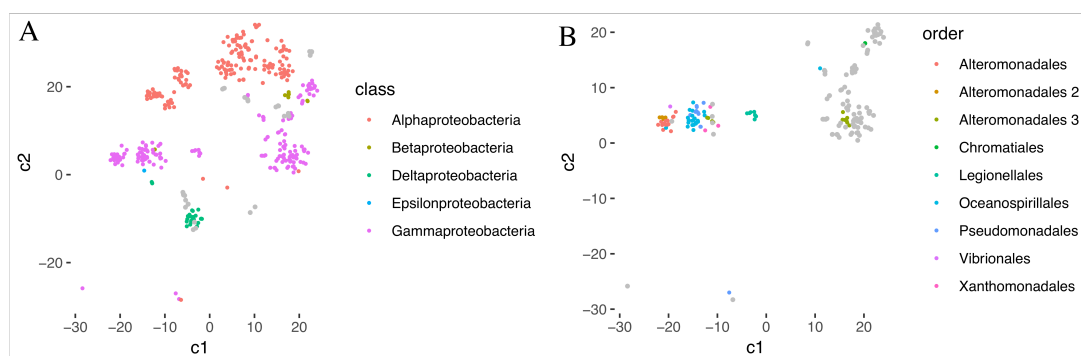


Figure 3: Supplement. Genome vectors cluster hierarchically by taxonomic rank. **(A)** The genome vectors of phylum *Proteobacteria* (pink in Figure 2, A) are labelled according to taxonomic class, and a subset of those vectors (pink) was then labelled by order (according to *Delmont et al.*). **(B)** As was the case for phyla, clusters represent distinct taxonomic entities. At the level of order, many MAGs could not be labelled in the original study, possibly because certain marker genes were missing (grey). However, their proximity to genomes with known taxonomy is clearly informative. Note for example the grey points around the order *Alteromonadales 3* (yellowish green), which could be plausibly grouped with it.

172 (Table 3)⁵⁶.

Table 1: Supplement. Domains found in the neighborhood of the DUF1537 protein family, later to be discovered to confer kinase function (PF07005, PF17042). All contextual domains identified by a previous study⁵³ can be retrieved from the domain embedding by their high *cosine similarity* to the query vector.

domains	cosine similarity	description
NBD_C	0.93	members of the DUF1537 family
Aldolase_II	0.63	class II aldolase
DctQ, DeoRC	0.53, 0.57	substrate binding proteins of TRAP transporters
KdgT, GntP_permease	0.60, 0.61	permease components of the TRAP transporters
RuBisCO_large	0.56	ribulose 1,5-bisphosphate carboxylase/ oxygenase
PdxA	0.56	4-hydroxy-l-threonine 4-phosphate dehydrogenase

Table 2: Supplement. Pairwise comparison of three MAGs which show low pairwise nucleotide (Jaccard) similarity but high functional (cosine) similarity (see also Figure 2, D). Note how functional similarity is higher than simple protein domain overlap, because it considers the context of individual domains as well.

MAG pair	nucleotide sim.	functional sim.	domain overlap
m05, m40	0.10	0.95	0.83
m05, m42	0.08	0.93	0.70
m40, m42	0.48	0.93	0.71

Table 3: Supplement. Case study MAGs and their closest assembled genomes in NCBI by nucleotide similarity.

MAG	closest assembly	nucleotide sim.	order
TARA_ANE_MAG_00005	UBA2589	0.862	Gemmatimonadales
TARA_RED_MAG_00040	UBA2960	0.744	Gemmatimonadales
TARA_ION_MAG_00042	UBA2960	0.518	Gemmatimonadales

173 **Genome vectors as inputs for machine learning tasks**

174 Many machine learning algorithms require vectors of numbers as their input. Genome vectors in
175 **nanotext** can be used as direct input to these algorithms without preprocessing or feature engineering.
176 Furthermore, sets of genome vectors can be composed to form new, meaningful topic vectors. A genus
177 or an environment can be described from its constituent genomes, e.g. by simply summing over them.
178 To illustrate this potential, we chose a complex learning tasks which has two components: Given a
179 genome assembly, we want to (1) recommend culture media in which the associated organism is likely to
180 grow, and (2) estimate the growth temperature required for culture from the community composition of
181 the environmental sample. More specifically, task (1) is a genotype-phenotype mapping (classification)
182 and we use a *fully connected neural net* to approach it. Task (2) is a regression for which we use
183 *gradient boosting trees*.

184 *Culture medium prediction*

185 Metagenomics is oftentimes the first window into a microbial environment. However, to study the
186 physiology of individual community members, cultivating a microorganism of interest is very important.
187 While most bacteria are still not culturable, there are recent high-throughput culturing efforts, which
188 are able to culture a surprisingly high number of bacteria⁵⁹. It is likely that many bacteria identified in
189 metagenomics are culturable, but it is difficult (without a deep niche-specific knowledge⁶⁰) to choose
190 among the thousands of medium recipes^{61,62}. Furthermore, many of these media are similar, in that
191 they are based upon another or share a significant number of ingredients. It is likely that many similar
192 media can be used to culture a single organism. The notion of “similar media” can be approached using
193 embeddings of medium ingredients⁶³. For each of the more than one thousand media in the catalogue
194 of the *German collection of microorganisms and cell cultures* (DSMZ), we trained a 10-dimensional
195 embedding vector. To predict medium vectors from genome vectors, we then had to link two databases,
196 namely the genome assemblies and annotations from the *Genome Taxonomy Database* (GTDB)¹² and
197 matching phenotype records from BacDive⁶².

198 Genome vectors can be used to accurately predict appropriate culture media for a given microorganism
199 based on its genome (Figure 4, A). This is perhaps unsurprising, because genome vectors represent a
200 genome’s functions which act as a constraint on growth conditions. We used a fully-connected neural
201 net to predict likely media from the catalogue of the DSMZ. Because the result is a medium vector,
202 we can search for similar media using cosine similarity. This provides a good starting point for culture
203 experiments. A common-sense baseline is to always predict the most common label of the data set
204 (medium no. 514), which would result in an accuracy of 0.17, i.e. medium no. 514 represents 17% of

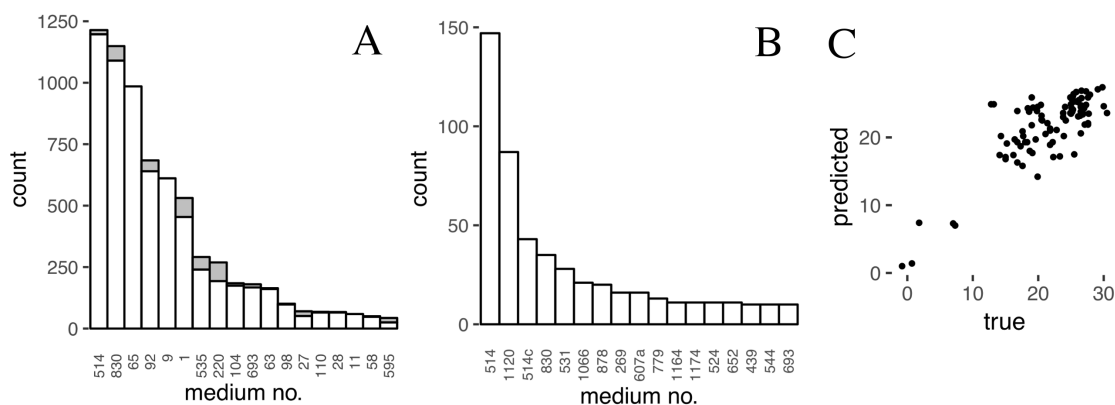


Figure 4: Prediction tasks. **(A)** Prediction of culture media from genomes. Classification task for genotype-phenotype mapping, namely predicting the culture medium for the associated microorganism of a given MAG. Shown is a stacked histogram of the culture media in the BacDive database (x-axis) and their count (y-axis). White bars indicate correct predictions, i.e. the target medium is in the top-10 list of closest media compared to the predicted vector. Grey bar fractions indicate false predictions. Only the 20 most common media in the database are displayed on the x-axis. **(B)** Predicted top media for Tara MAGs. The most common media (excluding their variants) in the prediction set are no. 514 (“Bacto Marine Broth”), no. 1120 (“PYSE Medium”) – e.g. used to study *Colwellia maris* isolated from seawater⁵⁷, no. 830 (“R2A Medium”) – developed to study bacteria which inhabit potable water⁵⁸, no. 1066 (“Marinobacter Lutaensis Medium”), no. 878 (“Thermus 162 Medium”), no. 269 (“Acidiphilium Medium”) and no. 607 (“M13 Verrucomicrobium Medium”) – which includes artificial seawater as an ingredient. All these media are representatives of a “marine topic” and plausible starting media for the organisms associated with the MAGs. **(C)** Inferring the water temperature of the environment for a given set of genomes (regression task). The ten most abundant MAGs from each Tara sampling location (n=93) were used to infer and sum across genome vectors. The resulting aggregate vector was used as input to a *Gradient Boosting Tree* classifier. Water temperature is predicted with an R^2 of 0.66. The dataset is very biased towards moderate temperatures, which likely reduces the predictive accuracy.

205 the media data. A prediction is classified correctly, if the target medium is in the first (1, 10) closest
206 media by cosine similarity, analogous to a common evaluation scheme in multi-class image labelling
207 tasks¹⁵. On the test set, our model obtains a top-1-accuracy of 63.5% and a top-10-accuracy of 82.5%
208 (Figure 4, A). On the Tara MAGs for which *Delmont et al.* could assign a genus, we obtained a
209 top-1-accuracy of 50% and a top-10-accuracy of 73.2% (Figure 4, B). The lower accuracy on the Tara
210 data is likely due to genomes without a close representative in the training data.

211 To further assess how well the model generalizes to unseen genome-media pairs, we investigated two
212 cyanobacterial Tara MAGs, which had their genus annotated by *Delmont et al.*, but for which no
213 representative is recorded in BacDive: TARA_ION_MAG_00012 is an MAG that corresponds to the genus
214 *Prochlorococcus*. For this organism, there exist established culture media such as “Artificial based
215 AMP1 Medium”⁶⁴. We were interested in whether our model could predict a similar medium, which
216 could then serve as a starting point for experimentation, were the media in current use unknown. We
217 labelled the AMP1 ingredients according to the protocol established by the KOMODO media database⁶¹
218 and then inferred the target medium vector by summing over the ingredient vectors. Surprisingly,
219 one of the top 10 media predicted for the *Prochlorococcus* MAG – no. 737, “Defined Propionate
220 Minima Medium” (DPM) – has a cosine similarity of 0.979 to the target AMP1 medium. Half of the
221 AMP1 medium ingredients can be found in DPM medium, including vital trace elements. Several
222 non-overlapping ingredients are part of buffers, and can likely be replaced by similar but distinct
223 ingredients. Because our medium embedding can represent such “synonyms”, the AMP1 and DPM
224 media are in fact more similar than they appear from shared ingredients alone. A similar generalization
225 of the medium prediction model can be observed for Tara MAG TARA_ASW_MAG_00003 of the genus
226 *Cyanothece*, which has received considerable attention due to its biotechnological potential⁶⁵. We again
227 encode a common culture medium for this genus – “ASP 2 Medium”⁶⁶ – as a medium vector. The
228 predicted medium based on the *Cyanothece* genome is no. 630, “Modified Thermus 162 Medium”, with
229 a cosine similarity of 0.98 and again a considerable overlap of ingredients.

230 *Water temperature prediction*

231 Genome vectors can be aggregated into new vectors which represent “topic summaries”. Aggregate
232 genome vectors of microbial communities can predict environmental properties. We use the most
233 abundant 10 MAGs in each of the 93 Tara sampling locations to predict the water temperature at
234 each respective sampling site, which is known from the Tara expedition’s metadata^{3,7}. Besides the fact
235 that the sample size is relatively small and the distribution skewed towards moderate temperatures,
236 we predict the correct water temperature with an R^2 of 0.66 (Figure 4, C).

237 Discussion

238 In this paper, we showed that protein domain and genome embeddings capture many functional aspects
239 of the underlying organism. The main assumption of our approach is that the *function* of a genome can
240 be abstracted as a sequence of protein domains. Much like words determine the topic of a document,
241 protein domains act as atomic units of “meaning” that describe the functions of a genome.

242 This view of function is very reductive, and much more comprehensive definitions exist¹. For example,
243 we do not consider functional RNAs⁶⁷ or functions that emerge from an interplay of different members
244 of an ecosystem^{68,69}. However, our results suggest that this reduced definition of function captures
245 many aspects that are already useful, e.g. for assigning taxa or genotype-phenotype mappings. This
246 success might also be related to our focus on bacteria, where many functions are protein-mediated and
247 the functional mechanisms are much simpler than in eukaryotes. We also completely omit archaea and
248 viruses in this study. However, the embedding model we provide with **nanotext** can be easily extended
249 by including said functional groups in the training corpus.

250 To expand the corpus with more (non-bacterial) genomes, a major bottleneck is the annotation step.
251 Currently most approaches are based on *Hidden Markov Models* (HMMs)^{70,71}, which scale poorly
252 to hundreds or even thousands of genomes. Recently, faster homology-based approaches have been
253 proposed⁷². It would be interesting to replace protein domain HMMs with homology-based protein
254 clusters, generated from large collections of metagenomic data such as the *Soil Reference Catalog*
255 (SRC), a catalog assembled from 640 soil metagenomes with two billion protein sequences¹⁰. With
256 such a large number of sequences, one would need to carefully calibrate the vocabulary size, i.e. the
257 number of protein clusters for the embedding. The **nanotext** embedding was trained with a corpus-
258 to-vocabulary ratio of $10^4 : 1$. To put this into perspective, current corpora in *Natural Language*
259 *Processing* (NLP) have a ratio above $10^5 : 1$ and well above 100 billion tokens for a vocabulary of
260 about one million words (the English language). Since even billion-scale vector collections can be
261 similarity searched efficiently, scaling to more genomes in the **nanotext** model is not problematic⁷⁴.
262 One further advantage of a vocabulary compiled from protein clusters would be the inclusion of many
263 unknown proteins in the embedding, which – albeit being unknown – could still be used in predictive
264 tasks. Corpora based on metagenomes would further reduce the bacterio-centric bias inherent in our
265 approach, by for example including viral proteins.

266 For training the embedding models, we used the **Word2Vec** algorithm³⁶ and its extension to
267 documents³⁹. **Word2Vec** is a special case of exponential family embeddings³⁵, and other embedding
268 methods could be better suited. For the culture medium embeddings for example, a *market basket*

269 *embedding* might be more appropriate. Domain vectors could be further enriched by “subword
270 information”^{38,75,76} i.e. by including nucleotide sequences in the model for inference of out-of-
271 vocabulary words. Embeddings could even be linked across modalities⁷⁷. Note that `Word2Vec` only
272 learns context in a narrow window – of in our case size 10 – and thus cannot learn long-range
273 interactions. However, this is not necessarily a limitation: The embeddings can be used as input for
274 routines that explicitly focus on such long-range interactions. Besides these potential improvements,
275 our embedding model already captures a surprising number of precise and subtle functional properties
276 because it is context-aware, which other metrics like *percentage domain overlap* are not.

277 We showed, that genome embeddings capture functional and by extension taxonomic properties of
278 the underlying genomes. It would be interesting to extend this work by creating a purely “functional
279 taxonomy”, i.e. one based only on genome vectors. Such an approach would assign taxa based on
280 whether certain genes were present or not, also known as *gene exclusivity*⁷⁸. By extension, it should
281 be possible to explore pangenomes using genome vectors. For example, we expect genera with an
282 open pangenome such as *Klebsiella* to present more genome vector variance than genera with closed
283 pangenomes such as *Chlamydia*⁷⁹.

284 Functional similarity-based pangenome studies could further be complemented with nucleotide simi-
285 larity search. This combination offers orthogonal viewpoints on the relatedness of organisms, with
286 potentially higher resolution than currently possible.

287 We also illustrated how downstream machine learning tasks benefit from embeddings as input. Not
288 only are embedding vectors convenient mathematical objects. Multiple embedding vectors can be com-
289 bined to represent e.g. individual genera or bacterial communities, which can then be used to create
290 genotype-phenotype mappings. We illustrated this by predicting likely culture media for assembled
291 genomes. Surprisingly, the notion of embedding similarity allows our predictive model to generalize
292 to genomes and media that were neither part of the training nor test data. Because only very lim-
293 ited data exists where genome assemblies are directly linked to culture media, we had to create a
294 genus-based mapping between the `AnnoTree` genome collection²⁹ and the `BacDive` database⁶². This
295 compromise likely reduces the predictive power of the learned model. However, as several strain collec-
296 tions started to whole-genome sequence their inventory – such as the DSMZ and the *Japan Collection*
297 *of Microorganisms* (JCM, http://jcm.brc.riken.jp/en/genomelist_e) – we can expect a much more
298 accurate genotype-phenotype mapping when methods such as `nanotext` are applied.

299 More generally, learning algorithms can become much more efficient when using embeddings as input,
300 because the algorithms can focus on the actual learning task and need not learn the “semantics” of the
301 problem in parallel. If for example we used raw nucleotide sequences as input to a learning algorithm,

302 it would have to learn concepts such as synonymous SNPs, which embeddings have already encoded.
303 Thus, embeddings reduce the amount of training data required and given a dataset of the same size
304 will oftentimes result in faster, better learning. If needed, pretrained embeddings can be additionally
305 trained on a downstream domain-specific learning task, e.g. as an embedding layer in a neural net. The
306 machine learning models we used are very basic, and could in the future be replaced by more powerful
307 models such as *Siamese neural nets*⁸⁰ and/ or optimized using e.g. alternative loss functions⁸¹.

308 In conclusion, we showed that protein domain and genome embeddings capture significant aspects of
309 a genome's functions, both on the level of domains as well as genomes, enabling a "taxonomy-free
310 taxonomy". They are well suited for subsequent machine learning tasks and solve the "curse of high
311 dimensionality" of previous approaches based on sparse encodings. As representations of function,
312 they have several useful properties, in that they are composable, well-formatted and insensitive in
313 light of incompleteness of the underlying assembly. Especially metagenomic areas such as taxonomic
314 classification, biomining and phenotype prediction can benefit from **nanotext**.

315 **Methods**

316 **Annotation of Tara genomes**

317 We annotated protein domains for a collection of 957 MAGs⁷ using HMMER (`hmmsearch --cut_ga,`
318 `v3.2.1`)⁷⁰ against the Pfam database (v32)¹⁹. We then removed domains with an E-value above 10^{-18}
319 and with a coverage below 35%. A Snakemake⁸² workflow implementation can be found in the project
320 repository.

321 **Estimation of nucleotide distance using MinHash**

322 To estimate average nucleotide identity between pairs of genomes we used the MinHash algorithm^{56,83} as
323 implemented in sourmash (<https://github.com/dib-lab/sourmash>)⁸⁴. To generate MinHash signatures
324 from genomes, we chose a sketch size of 500 and a k-mer size of 31.

325 **Training of functional embeddings**

326 We combined two large collections of bacterial genome annotations into one corpus. First we included
327 the complete AnnoTree collection²⁹ based on the *Genome Taxonomy Database* (GTDB) ($n = 23936$,
328 release 83)¹². Second, from the EnsemblBacteria database we randomly sampled five genomes for each
329 species ($n = 8667$, release 41)⁸⁵. The sampling balances the dataset; otherwise medically important
330 bacteria would dominate the resulting corpus (<https://osf.io/pjf7m/>). Each line in the corpus is the
331 sequence of PFAM protein domains on a contig. Strand information is not preserved. We did not
332 perform any additional filtering of the protein domains. We trained embeddings on a corpus of 31730
333 genomes with a total of about 145 million domains.

334 We obtained word vectors using the Word2Vec³⁶ algorithm for all words in our corpus' vocabulary of
335 10879 domains, which is about 60% of the total number of domains in the Pfam database (v32)¹⁹. Note
336 that not all domains in Pfam are bacterial, and we further excluded protein domains that did not occur
337 in the corpus at least three times. We trained a document topic model using the Doc2Vec algorithm³⁹
338 with a window size of 10 and a linearly decreasing learning rate (0.025 to 0.0001) over 10 epochs using
339 the *distributed bag of words* (PV-DBOW) training option as implemented in Gensim⁸⁶. The result was
340 a 100-dimensional vector. The similarity of any two genome vectors in the collection can be evaluated
341 using cosine similarity, with a range from -1 (no similarity) to 1 (identical). To infer genome vectors
342 for new genomes, we concatenated the protein domain sequences of all contigs and then used 200

343 iterations for inference. This resulted in stable vector estimates with a pairwise cosine distance < 0.01 .
344 For the SOMO evaluation task (see results) we withheld 873 randomly selected genomes (3%) from
345 training, to validate the embedding model.

346 **Training of media embeddings**

347 To quantify how similar any pair of culture media was, we created a media embedding. Such a
348 representation has an advantage over using the name or ID of a medium in learning tasks, because
349 many media are very similar, such as when an organism-specific medium is an extension of a base
350 medium. Using an ID, we would create a high-dimensional, one-hot-encoded vector to represent the
351 medium. This vector would be very sparse, with 1 in the index position of a given medium and 0
352 everywhere else. The current media collection of the DSMZ lists over 1500 media, so any learning
353 algorithm would have problems with the number of dimensions.

354 To reduce the number of media, we treat a medium recipe as a sequence of ingredients and used
355 `Word2Vec`³⁶ to create a latent representation in the form of a 10-dimensional vector, similar in idea
356 to embedding cooking recipes (<https://bit.ly/2kesqbC>) or diets⁶³. The DSMZ media are not easily
357 parsable and contain many non-unique ingredient tags such as “beef extract” and the synonymous
358 “meat extract”. Therefore we used preprocessed data from the KOMODO database of known media⁶¹. To
359 download all 3637 recipes, we used a custom crawling script (`scrape_komodo.py`). Note that some
360 current additions to the DSMZ media list do not figure in the KOMODO database. From each recipe we ex-
361 tracted a list of ingredients⁶¹. We excluded water (`SEED-cpd00001###`) and agar (`SEED-cpd13334###`)
362 because these ingredients are highly redundant and would act as noise during training. We embedded
363 the ingredients using `Word2Vec` with a window size of 5 and a learning rate as described above over
364 100 epochs using negative sampling of 15 words per window. To make sure that pairs of media ingredi-
365 ents could occur in the same window, we augmented the data set by shuffling each ingredient list 100
366 times⁸⁷. The result is a 10-dimensional vector for each media ingredient. To create culture medium
367 embeddings, we summed across the embedding vectors for all ingredients in a medium.

368 The similarity of any two DSMZ media could then be compared using cosine similarity. For example,
369 the closest media to medium no. 1 are medium no. 306 (0.99) and no. 617 (0.99), one adding *yeast*
370 *extract* and the other *NaCl* to medium no. 1; an ID-based representation would treat these media as
371 distinct, although they are near identical. Indeed, medium no. 617 and 953 have identical ingredients,
372 which is reflected by a cosine similarity of 1.

373 Embeddings are useful as input to learning algorithms only if they position similar entities in similar

374 vector space, i.e. if similar entities cluster. We therefore visualized the media vector space using t-SNE
375 (Figure 5). Indeed, similar media cluster and thus enable learning algorithms to discriminate media
376 classes. For downstream machine learning tasks, the vector representation has two major advantages:
377 It reduces the dimensionality of the media representation by 2 orders of magnitude, from one-hot-
378 encoding of more than one thousand media to a 10-dimensional vector. Another advantage is that
379 any predicted medium (see results) can suggest n similar media as starting point, instead of just one.
380 While this might seem inexact, we think it offers much more information about culturing previously
381 uncultured organisms, as a wider range of media can be explored and mixed.

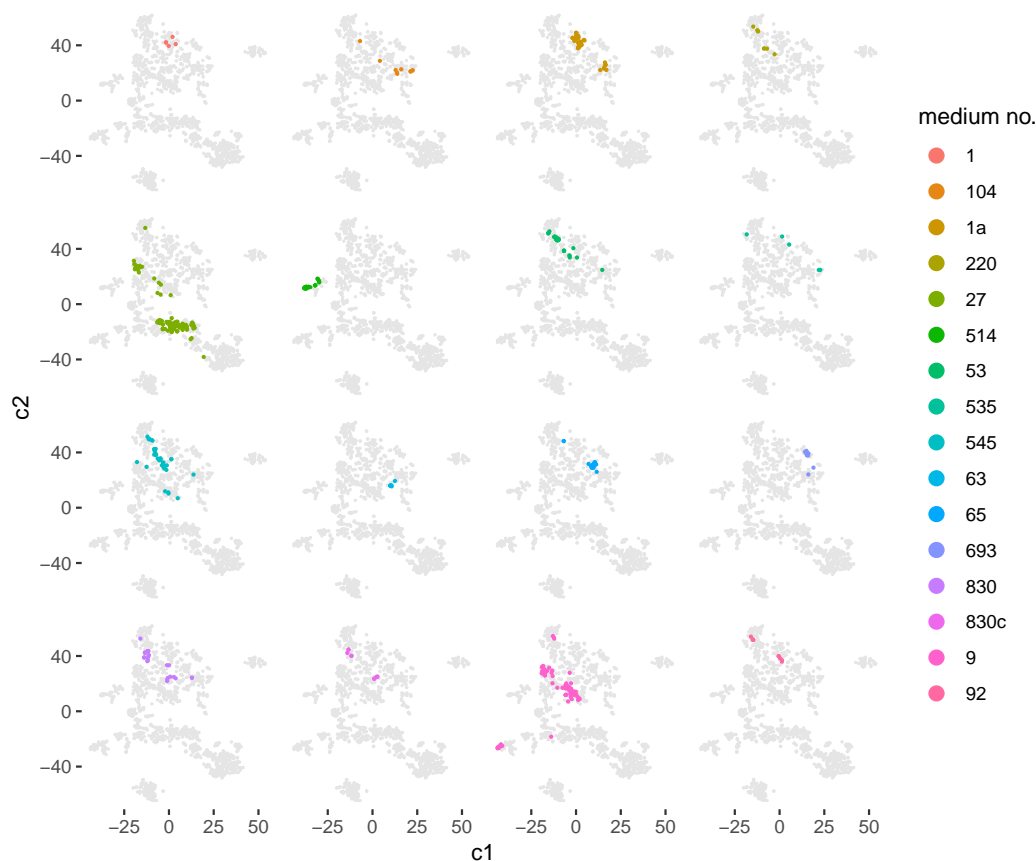


Figure 5: Supplement. Culture medium embedding. We used t-SNE to project the associated 10-dimensional embedding vector into the plane (grey points). We colored all media with more than 0.95 cosine similarity to the top 16 most common DSMZ media in the BacDive database. We observe clear clusters of similar media. These clusters can be used by learning algorithms to discriminate media classes. Also note how near-identical media such as no. 830 and no. 830c are embedded in near identical vector space, which acts as a negative control to validate the embedding model.

382 **Linking AnnoTree genome assemblies to BacDive culture media**

383 To predict a medium (vector) from a genome (vector) we needed to create a training set that matches
384 the two. The **BacDive** database from the DSMZ holds taxonomic and phenotypic information includ-
385 ing culture media for currently over 60 thousand strains⁶². However, these strains do not directly
386 correspond to genomes in the **AnnoTree** collection^{12,29}. To link these two, we had to pair records using
387 taxonomy at the rank of genera.

388 **Machine learning**

389 *Culture medium prediction*

390 For the medium prediction task, we used a multi-layer fully connected neural network. We selected the
391 training data as follows: For each genus used to link the two databases, we first sampled records from
392 **BacDive** at the genus level. Because this data is highly skewed towards medically relevant genera such
393 as *Mycobacterium*, we randomly selected a maximum of 100 records per genus to balance the training
394 data. As target y , we used the embedding vector of the the most common culture medium in **BacDive**
395 at the genus level. For the same genus we then randomly sampled a genome vector from **nanotext**,
396 which we used as input X . We had to use the most common medium and not sample from these media
397 as we did for the genome input, because many **BacDive** records hold a list of possible culture media
398 with very different recipes and by extension very distant media embeddings. For example, there are
399 two media records for the genus *Rubrimonas*, no. 13 and 514, with a cosine similarity of 0.48 – given
400 that our data set is small, the learning algorithm was not able to learn this complex mapping.

401 We repeated this process 10 times to augment our dataset. Data augmentation is a common practice
402 when training neural nets. It enables the training of more complex models, which then generalize
403 better. Using data augmentation, we can circumvent the need to collect more data by varying the
404 input slightly. For images this typically means flipping images horizontally or generating new training
405 images by selecting only a subset of pixels. In seminal work on the **ImageNet** challenge for example, the
406 original data was augmented 2048 times¹⁵. We used a total of 73916 genom-media pairs for training,
407 optimized hyperparameters on a validation set of 3891 (5%) and tested the final model on a holdout set
408 of size 8646 (10%). The neural net architecture consisted of three fully connected layers with (512, 128,
409 64) nodes. Before applying the non-linear transformation (rectified linear units, ReLU), we normalized
410 the batches of size 128. After each layer we applied Dropout (0.5, 0.3, 0.1). The output layer had 10
411 nodes to represent a culture medium vector with 10 latent elements, which were activated with a linear
412 transformation. We optimized a cosine similarity loss of the output medium vector with the target

413 medium vector using the Adam optimizer with a learning rate of 10^{-2} over the course of 10 epochs.
414 Because we used a cosine similarity loss, we did not rescale (X, y) before training. We implemented
415 the model using the deep learning library Keras (<https://keras.io>).

416 *Water medium prediction*

417 For the water temperature prediction task we used a *Gradient Boosting Trees* (GBT) regressor⁸⁸. For
418 each of the 93 sampling sites in the Tara dataset, we averaged the genome vectors of the 10 most
419 abundant MAGs, where abundance was estimated using the relative number of reads that belonged
420 to any MAG at the given sampling site⁷. Our target variable was the recorded temperature for this
421 site (see supplementary information in *Delmont et al.*). We used grid search to optimize the GBT
422 parameters (learning rate: 0.05, maximum depth: 4, maximum percentage of features used during
423 iterations: 30%, minimum number of samples per leaf: 3). The final model is an ensemble of 3000
424 trees. Because the number of samples was small compared to the input dimensions, we used leave-one-
425 out cross-validation (LOOCV) to make predictions. The model was implemented using the machine
426 learning library Sklearn⁸⁹.

427 **Code availability**

428 All relevant resources to reproduce the major results in this article have been deposited in a dedicated
429 **nanotext** repository (<https://github.com/phiweger/nanotext>). This includes source code, protein do-
430 main and genome embeddings as well as preprocessing workflows. The corpus we trained **nanotext**
431 on is also made available (<https://osf.io/pjf7m/>).

432 **Acknowledgments**

433 The authors thank Donovan Parks for providing the AnnoTree protein domain annotations.

434 **References**

- 435 **1** Stadler, P. F. *et al.* *Theory Biosci.* 128, 165–170 (2009)
- 436 **2** Doolittle, W. F. *Genome Biol.* 19, 223 (2018)
- 437 **3** Pesant, S. *et al.* *Sci Data* 2, 150023 (2015)
- 438 **4** Parks, D. H. *et al.* *Nat Microbiol* 2, 1533–1542 (2017)
- 439 **5** Tully, B. J. *et al.* *bioRxiv* 162503 (2017)
- 440 **6** Stewart, R. *et al.* *bioRxiv* 162578 (2017)
- 441 **7** Delmont, T. O. *et al.* *Nat Microbiol* 3, 804–813 (2018)
- 442 **8** Stewart, R. D. *et al.* *bioRxiv* 489443 (2018)
- 443 **9** Qin, J. *et al.* *Nature* 464, 59–65 (2010)
- 444 **10** Steinegger, M. *et al.* *bioRxiv* 386110 (2018)
- 445 **11** Tatusov, R. L. *et al.* *Nucleic Acids Res.* 28, 33–36 (2000)
- 446 **12** Parks, D. H. *et al.* *Nat. Biotechnol.* 36, 996–1004 (2018)
- 447 **13** Valenzuela, L. *et al.* *Biotechnol. Adv.* 24, 197–211 (2006)
- 448 **14** Pascal, V. *et al.* *Gut* 66, 813–822 (2017)
- 449 **15** Krizhevsky, A. *et al.* in *Advances in neural information processing systems 25* (eds. Pereira, F.,
450 Burges, C. J. C., Bottou, L. & Weinberger, K. Q.) 1097–1105 (Curran Associates, Inc., 2012)
- 451 **16** Langille, M. G. I. *mSystems* 3, (2018)
- 452 **17** Doolittle, W. F. *et al.* *Biol. Philos.* 32, 5–24 (2017)
- 453 **18** Heintz-Buschart, A. *et al.* *Trends Microbiol.* 26, 563–574 (2018)
- 454 **19** Finn, R. D. *et al.* *Nucleic Acids Res.* 44, D279–85 (2016)
- 455 **20** Alborzi, S. Z. *et al.* *BMC Bioinformatics* 18, 107 (2017)
- 456 **21** Vogel, C. *et al.* *Curr. Opin. Struct. Biol.* 14, 208–216 (2004)

- 457 **22** Tordai, H. *et al.* *FEBS J.* 272, 5064–5078 (2005)
- 458 **23** Marsh, J. A. *et al.* *Genome Biol.* 11, 126 (2010)
- 459 **24** Illergård, K. *et al.* *Proteins* 77, 499–508 (2009)
- 460 **25** Holmes, E. C. (OUP Oxford, 2009)
- 461 **26** Zhu, C. *et al.* *PLoS Comput. Biol.* 11, e1004472 (2015)
- 462 **27** Zhu, C. *et al.* *Nucleic Acids Res.* 46, D535–D541 (2018)
- 463 **28** Weimann, A. *et al.* *mSystems* 1, (2016)
- 464 **29** Mendler, K. *et al.* *bioRxiv* 463455 (2018)
- 465 **30** Blin, K. *et al.* *Nucleic Acids Res.* 45, W36–W41 (2017)
- 466 **31** Terrapon, N. *et al.* *Nucleic Acids Res.* 46, D677–D683 (2018)
- 467 **32** Gordon, S. P. *et al.* *PLoS One* 10, e0132628 (2015)
- 468 **33** Burkhardt, D. H. *et al.* *Elife* 6, (2017)
- 469 **34** Hinton, G. E. *et al.* in (eds. Rumelhart, D. E., McClelland, J. L. & PDP Research Group, C.)
470 77–109 (MIT Press, 1986)
- 471 **35** Rudolph, M. R. *et al.* (2016)
- 472 **36** Mikolov, T. *et al.* in *Advances in neural information processing systems 26* (eds. Burges, C. J. C.,
473 Bottou, L., Welling, M., Ghahramani, Z. & Weinberger, K. Q.) 3111–3119 (Curran Associates, Inc.,
474 2013)
- 475 **37** Pennington, J. *et al.* in *In EMNLP* (2014)
- 476 **38** Bojanowski, P. *et al.* (2016)
- 477 **39** Le, Q. V. *et al.* (2014)
- 478 **40** Blei, D. M. *Commun. ACM* 55, 77–84 (2012)
- 479 **41** Asgari, E. *et al.* *PLoS One* 10, e0141287 (2015)
- 480 **42** Du, J. *et al.* *bioRxiv* 286096 (2018)

- 481 **43** Yang, K. K. *et al. Bioinformatics* 34, 2642–2648 (2018)
- 482 **44** Hamid, M.-N. *et al. Bioinformatics* (2018)
- 483 **45** Jaeger, S. *et al. J. Chem. Inf. Model.* 58, 27–35 (2018)
- 484 **46** Kimothi, D. *et al.* (2016)
- 485 **47** Ng, P. (2017)
- 486 **48** Asgari, E. *et al. Bioinformatics* (2018)
- 487 **49** Asgari, E. *et al. Bioinformatics* 34, i32–i42 (2018)
- 488 **50** Schnabel, T. *et al. Proceedings of the 2015 Conference on Empirical Methods in Natural Language*
489 *Processing* 298–307 (2015)
- 490 **51** Conneau, A. *et al.* (2018)
- 491 **52** Maaten, L. van der. *J. Mach. Learn. Res.* 15, 3221–3245 (2014)
- 492 **53** Zhang, X. *et al. Proc. Natl. Acad. Sci. U. S. A.* 113, E4161–9 (2016)
- 493 **54** O’Leary, N. A. *et al. Nucleic Acids Res.* 44, D733–45 (2016)
- 494 **55** Campbell, B. J. *et al. Proc. Natl. Acad. Sci. U. S. A.* 108, 12776–12781 (2011)
- 495 **56** Ondov, B. D. *et al. Genome Biol.* 17, 132 (2016)
- 496 **57** Wannicke, N. *et al. FEMS Microbiol. Ecol.* 91, (2015)
- 497 **58** Sandle, T. *PDA J. Pharm. Sci. Technol.* 58, 231–237 (2004)
- 498 **59** Browne, H. P. *et al. Nature* 533, 543–546 (2016)
- 499 **60** Ark, K. C. H. van der *et al. Microb. Biotechnol.* 11, 476–485 (2018)
- 500 **61** Oberhardt, M. A. *et al. Nat. Commun.* 6, 8493 (2015)
- 501 **62** Reimer, L. C. *et al. Nucleic Acids Res.* (2018)
- 502 **63** Tansey, W. *et al.* (2016)
- 503 **64** Moore, L. R. *et al. Limnol. Oceanogr. Methods* 5, 353–362 (2007)
- 504 **65** Bandyopadhyay, A. *et al. MBio* 2, (2011)

- 505 **66** Welsh, E. A. *et al. Proc. Natl. Acad. Sci. U. S. A.* 105, 15094–15099 (2008)
- 506 **67** Waters, L. S. *et al. Cell* 136, 615–628 (2009)
- 507 **68** Sunagawa, S. *et al. Science* 348, 1261359 (2015)
- 508 **69** Roux, S. *et al. Nature* 537, 689–693 (2016)
- 509 **70** Eddy, S. R. *PLoS Comput. Biol.* 7, e1002195 (2011)
- 510 **71** Hauser, M. *et al. Bioinformatics* 32, 1323–1330 (2016)
- 511 **72** Mahlich, Y. *et al. Bioinformatics* 34, i304–i312 (2018)
- 512 **73** Steinegger, M. *et al. Nat. Commun.* 9, 2542 (2018)
- 513 **74** Johnson, J. *et al.* (2017)
- 514 **75** Joulin, A. *et al.* (2016)
- 515 **76** Wu, L. *et al.* (2017)
- 516 **77** Salvador, A. *et al.* in *2017 IEEE conference on computer vision and pattern recognition (CVPR)*
517 3068–3076 (2017)
- 518 **78** Wright, E. S. *et al. BMC Genomics* 19, 724 (2018)
- 519 **79** McInerney, J. O. *et al. Nat Microbiol* 2, 17040 (2017)
- 520 **80** Koch, G. *et al.* in *ICML deep learning workshop 2*, (2015)
- 521 **81** Wojke, N. *et al.* in *2018 IEEE winter conference on applications of computer vision (WACV)*
522 748–756 (2018)
- 523 **82** Köster, J. *et al. Bioinformatics* 28, 2520–2522 (2012)
- 524 **83** Broder, A. Z. in *Compression and complexity of sequences 1997. Proceedings* 21–29 (IEEE, 1997)
- 525 **84** Brown, C. T. *et al. The Journal of Open Source Software* (2016)
- 526 **85** Zerbino, D. R. *et al. Nucleic Acids Res.* 46, D754–D761 (2018)
- 527 **86** Řehůřek, R. *et al.* (University of Malta, 2010)
- 528 **87** Barkan, O. *et al.* (2016)

529 **88** Friedman, J. H. *Ann. Stat.* 29, 1189–1232 (2001)

530 **89** Pedregosa, F. *et al. J. Mach. Learn. Res.* 12, 2825–2830 (2011)